New Epoxy sugar based glucose derivatives as eco friendly corrosion inhibitors for the carbon steel in 1.0☐M HCl: Experimental and theoretical investigations

M. Rbaa, P. Dohare, A. Berisha, O. Dagdag, L. Lakhrissi, M. Galai, B. Lakhrissi, M. Ebn Touhami, I. Warad, A. Zarrouk

PII: S0925-8388(20)31312-8

DOI: https://doi.org/10.1016/j.jallcom.2020.154949

Reference: JALCOM 154949

To appear in: *Journal of Alloys and Compounds*

Received Date: 29 January 2020

Revised Date: 24 March 2020

Accepted Date: 25 March 2020

Please cite this article as: M. Rbaa, P. Dohare, A. Berisha, O. Dagdag, L. Lakhrissi, M. Galai, B. Lakhrissi, M.E. Touhami, I. Warad, A. Zarrouk, New Epoxy sugar based glucose derivatives as eco friendly corrosion inhibitors for the carbon steel in 1.0☐M HCl: Experimental and theoretical investigations, *Journal of Alloys and Compounds* (2020), doi: https://doi.org/10.1016/j.jallcom.2020.154949.

CRediT authorship contribution statement

M. Rbaa : Investigation, Writing - original draft.
P. Dohare : Investigation, Writing - original draft.
A. Berisha : Investigation, Writing - original draft.
O. Dagdag : Investigation, Writing - original draft.
L. Lakhrissi : Investigation, Writing - original draft.
M. Galai : Investigation, Writing - original draft.
B. Lakhrissi : Conceptualization, Writing - original draft, Writing - review & editing.
M. Ebn Touhami: Conceptualization, Writing - original draft, Writing - review & editing.
I. Warad : Conceptualization, Writing - original draft, Writing - review & editing.
A. Zarrouk : Conceptualization, Writing - original draft, Writing - review & editing.

New Epoxy sugar based glucose derivatives as eco friendly corrosion inhibitors for the carbon steel in 1.0 M HCl: Experimental and theoretical investigations

M. Rbaa [a], P. Dohare [b], A. Berisha [c], O. Dagdag [a], L. Lakhrissi [a], M. Galai [d], B. Lakhrissi [a], M. Ebn Touhami [d], I. Warad [e], A. Zarrouk [f]

[a] Laboratory Agro-Resources, Polymers and Process Engineering, Department of Chemistry, Faculty of Sciences, Ibn Tofail University, PO Box 133, 14000, Kenitra, Morocco.
[b] Department of Chemistry, Indian Institute of Technology (BHU), Varanasi-221005, India.
[c] Department of Chemistry, Faculty of Natural and Mathematics Science, University of Prishtina, 10000 Prishtina, Kosovo.
[d] Laboratory of Materials Engineering and Environment: Modeling and Application, Faculty of Science, Ibn Tofail University BP. 133-14000, Kenitra, Morocco.
[e] Department of Chemistry and Earth Sciences, PO Box 2713, Qatar University, Doha, Qatar.
[f] Laboratory of Materials, Nanotechnology and Environment, Faculty of Sciences, Mohammed V University, Av. Ibn Battuta. B.P 1014, Rabat, Morocco.

✉ **Corresponding authors**

Prof. Abdelkader ZARROUK

E-mail: azarrouk@gmail.com

Phone: 00212665201397

http://orcid.org/0000-0002-5495-2125

Dr. Mohamed Rbaa

E-mail: mohamed.rbaa10@gmail.com.

Phone: 00212682988498

http://orcid.org/0000-0003-1235-890X

Abstract

In this study, we chose to synthesize new *sugar* based glucose derivatives as ecological corrosion inhibitors for carbon steel in acidic medium. The products obtained in the form of syrupy liquids, and the purity of obtained compounds was characterized by *NMR* spectroscopy analysis. The corrosion inhibition activities for both compounds were evaluated by electrochemical and rheological methods. Thus, the results of the experimental tests have been confirmed by theoretical studies (*DFT*, *MC* and *MD* simulations). The surface study of carbon steel has been characterized by the scanning electron spectroscopy (*SEM*). The gravimetric solutions were identified using UV-Vis spectroscopy and Inductively Coupled Plasma-Optical Spectroscopy (*ICP-OES*).

Keywords: Synthesis; Rheological methods; Eco friendly corrosion inhibitors; Electrochemical techniques; SEM; MD simulations.

1. Introduction

The assessment of corrosion of steel and the presentation of the solutions has been a question of great interest in most of the metal industrial sectors [1]. Therefore, improving the mechanical properties of these metals is of great interest in a wide range of disciplines. For a long time, researchers presenting solutions for this unwanted phenomenon, among the most cost-effective proposals presented are the protection from the organic or inorganic chemical inhibitors. In addition, the chemical inhibitors are very profitable for the corrosion inhibition of steel, especially in acidic media, like hydrochloric acid and sulfuric acid medium [2-10]. By way of example, we have found heterocyclic inhibitors which are effective in inhibiting corrosion of steel in an acid medium, such as *8-hydroxyquinoline* and its derivatives, *benzimidazole* derivatives, *quinoxaline* derivatives [11-13]. However, the problem of these heterocycles presents a little signs of both toxicity for the environment [14]. Also, the application of synthetic compounds as corrosion inhibitors is limited because of the increasing ecological awareness and strict environmental regulations as most of the traditional corrosion inhibitors are synthesized using expensive and toxic chemicals and solvents. In view of this, recently, Glucose and their derivatives are being used as corrosion inhibitors as they are available at the economic and commercial level [15]. Because of the natural and biological origin, they can be regarded as one of the greenest sources of the chemical compounds used as corrosion inhibitors. More so, the presence of numerous polar functional groups such as –OH further enhance their corrosion inhibition effectiveness by increasing their molecular size as well as increase solubility in the polar electrolytes. These polar functional groups can also serve as adsorption centers during the meta-inhibitor interactions. Looking the greenness of glucose and their derivatives along with their high protection efficiency, the synthesis, characterization and utilization in all fields of science and technology, including in the area of metallic corrosion inhibition should be further explored [16]. The ecological inhibitors have been the subject of many published studies for corrosion inhibition in acidic medium. In addition, the ecological inhibitors have two major advantages, the first effective corrosion inhibition and the second do not affect the environment [17]. The ecological inhibitors are of natural in origin, such as oils and seeds of medicinal plants, or of synthetic origin, such as *glucose*, *mannose* and *fructose* [18,19]. However, the advantage of sugar-based compounds remains the best ecological inhibitors because their degradations in the media always give basic molecules, which is the simple sugar (*glucose*, *mannose* or *fructose*). According to the literature, glucose and its derivatives are not toxic to nature and living beings. In addition, glucose is widely used in the hospitals field as a potential drug, especially in the form of syrup. In addition, glucose is used to prevent the crystallization of sugar, nougatine, boiled sweets, soft caramels, fruit pastes, gums and marshmallows [20,21].

In this work, we focused on the synthesis and presentation of newly synthesized glucose derivatives as ecological inhibitors of carbon steel in molar hydrochloric acid. The study of corrosion inhibiting power is approved using the rheological methods and electrochemical methods (impedance spectroscopy and potentiodynamic polarization). The experimental results have been confirmed by theoretical studies (calculates *DFT*, *MC* and *MD* simulations). The surface study of the carbon steel after the corrosion was characterized by the scanning electron spectroscopy (*SEM*). The gravimetric solutions were analyzed using *UV-Vis* spectroscopy and Inductively Coupled Plasma-Optical Spectroscopy (*ICP-OES*).

2. Material and methods

2.1. Chemical study

All instruments, reagents, and the used solvent for the preparation of these compounds have been published in a previous work [22]. The NMR spectra were carried out on a BRUKER AM 300 spectrometer operating in Fourier transform at the frequency of 300.13 MHz for ^{1}H

NMR and 75.47 MHz for ^{13}C NMR. The associated calculator is an Aspect 3000 using the BRUKER 1986 software (DI6R 861). The compound is dissolved in a proportion of 40 to 100 mg in 0.2 to 0.5 ml of deuterated solvent (DMSO). Tetramethylsilane (TMS) is used as a fictitious reference, different control tubes used to regularly calibrate the apparatus by fixing the SR (Spectrum Reference).

The synthesis of glucose-derived inhibitors was performed under specific conditions in five steps (**Figure 1**).

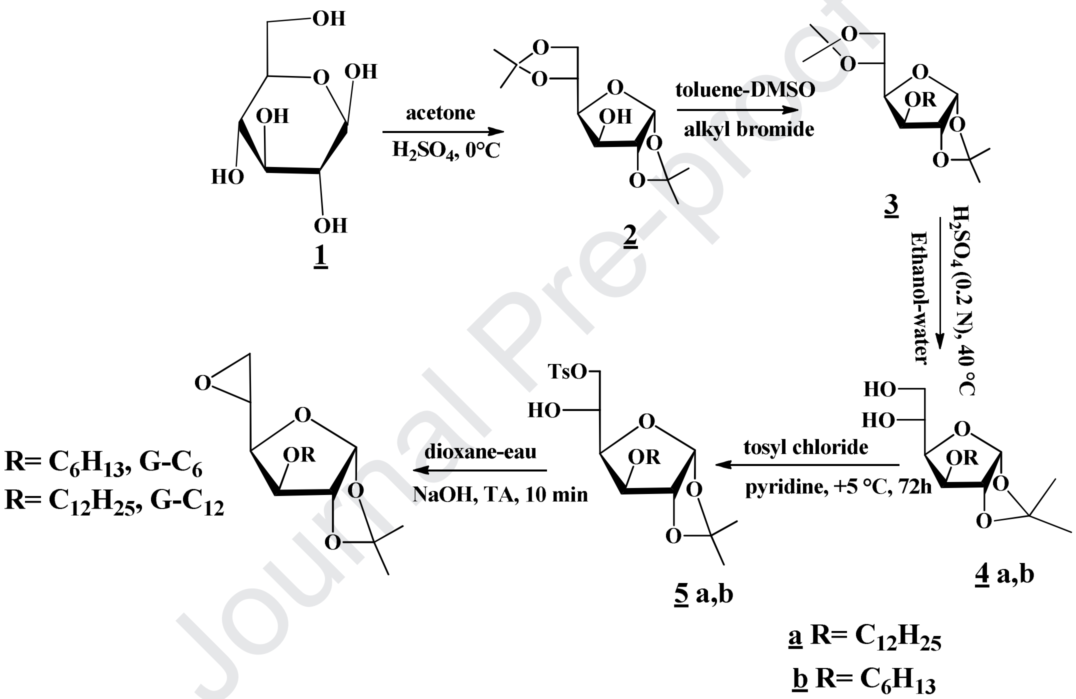

Figure 1. Synthesis of 5,6-anhydro-3-O-dodecyl-1,2-O-isopropylidene-α-D-glucofuranose (**G-C_{12}**) and 5,6-anhydro-3-O-hexadecyl-1,2-O-isopropylidene-α-D-glucofuranose (**G-C_6**)

General procedure for organic synthesis

To a solution of tosylated substrates (**<u>5</u>** a, b) (220 g L^{-1}) in the *dioxane-water* mixture (9: 1) were added 2.4 equivalent of *sodium hydroxide*. The reaction mixture is stirred for 1 h at room temperature and *TLC* monitors the reaction. After filtration, the reaction mediums are neutralized with a saturated aqueous solution of ammonium chloride and extracted twice with toluene. The combined organic phases are dried over sulfate of anhydrous sodium, filtered and the filtrate is evaporated under reduced pressure. The reaction crude is chromatographed on a column of silica gel (eluent gradient: hexane acetone) to give the compounds ***G-C$_6$*** and ***G-C$_{12}$*** in the form of syrupy liquids, whose structure and purity were later confirmed by ^{13}C and ^{1}H *NMR* spectroscopic analyzes.

2.2. Electrochemical and rheological test

The corrosion inhibition effect of the ***G-C$_6$*** and ***G-C$_{12}$*** on carbon steel corrosion in 1.0 M HCl first of all demonstrated using electrochemical methods. The electrochemical studies were carried out using conventional three electrode system in which platinum rod, saturated calomel and carbon steel specimen are used as a counter, reference and working electrodes, respectively. The electrochemical impedance spectroscopic (EIS) studies were carried out at OCP (Open Circuit Potential) in the frequency range of 100 KHz−100 mHz, with 10 points per decade. The EIS data were fitted in a suitable equivalent circuit to get values of polarization resistance (R_p).

Potentiodynamic polarization (PDP) studies on the corrosion of carbon steel in 1.0 M HCl with and without ***G-C$_6$*** and ***G-C$_{12}$*** were carried out by recording the anodic and cathodic Tafel curves in the potential range of -800 mV to -200 mV with respect to the potential of SCE (saturated calomel electrode) with a scan rate of 0.5 mV s^{-1}.

The inhibition efficiencies were calculated using following equations (1,2): respectively, for the potentiodynamic polarization and electrochemical impedance spectroscopy techniques.

$$\eta_{\mathrm{PP}} = \frac{i^{0}_{\mathrm{corr}} - i_{\mathrm{corr}}}{i^{0}_{\mathrm{corr}}} \times 100 \qquad (1)$$

i_{corr} and i^{0}_{corr} are the corrosion current density with and without the addition of inhibitors (***G-C$_6$*** and ***G-C$_{12}$***).

$$\eta_{\mathrm{EIS}} = \frac{R_{\mathrm{p}} - R^{0}_{\mathrm{p}}}{R_{\mathrm{p}}} \times 100 \qquad (2)$$

R_p and R_p^0 are the polarization resistance with and without the addition of inhibitors (***G-C₆*** and ***G-C₁₂***).

The material used in this study was a carbon steel with a chemical composition (in wt%) of C, 0.11; Si, 0.24; Mn, 0.47; Cr, 0.12; Mo, 0.02; Ni, 0.1; Al, 0.03; Cu, 0.14; Co, < 0.012; V, < 0.003; W, 0.06; Fe, balance. The steel samples were pre-treated prior to the experiments by grinding with emery paper SiC (120, 400, 600 and 1200); rinsed with distilled water, degreased in acetone in an ultrasonic bath immersion for 5 min, washed again with bidistilled water and then dried at room temperature before use. The acid solutions (1.0 M HCl) were prepared by dilution of an analytical reagent grade 37 % HCl with double distilled water. The concentration range of ***G-C₆*** and ***G-C₁₂*** employed in this study was 10^{-6} M to 10^{-3} M.

The rheological study has been detailed in another work that is already published [23].

2.3. Surface characterization

The surface morphology was studied using an SEM instrument (JOEL model JSM-5500 microscope). UV-Vis [Jenway ultraviolet-visible spectrophotometer (series 67)] technique was utilized to investigate the formed complexes.

2.4. DFT, Monte Carlo and Molecular Dynamic Simulations

The *DFT*, Monte Carlo (*MC*) and Molecular Dynamics (*MD*) and calculation were performed using Materials Studio 7.0 [24].

DFT calculations were performed using the DMol^3 software (within the Materials Studio). All electron calculations are employed for geometry optimization with the double numerical plus polarization basis set (DNP) [25]. The exchange-correlation energy is described by the Perdew–Burke–Ernzerhof functional within the generalized gradient approximation (GGA/PBE). All energy minima were characterized by performing a vibrational analysis to ensure the lack of imaginary frequencies [26].

For *MC* the interaction between iron surface and the inhibitor in the simulated corrosion media is approximated using the slab model of Fe (110) with periodic boundary conditions [using a Fe unit cell, cleaved at h k l (1 1 0) plane and expanded 10x10 with the addition of an 30 A vacuum layer at C axis) containing 700 water molecules/one inhibitor molecule (either ***G-C$_6$*** or ***G-C$_{12}$*** /25 hydronium+25 chloride ions. The Metropolis Monte Carlo method was used to evaluate the adsorption configurations [COMPASS II force field, (energy convergence tolerance of 2×10^{-5} kcal/mol, force convergence tolerance of 0.001 kcal/mol/A)] of the interaction between the molecules and the substrates.

The *MD* simulations with the Forcite Module (Materials Studio) were accomplished using COMPASS II (Condensed-phase Optimized Molecular Potentials for Atomistic Simulation Studies) force field with the atom charges assigned from GGA/PBE calculations [27]. Prior to the use of *MD* simulations, the slab model containing the corrosion media and the inhibitor molecule is optimized using the Smart optimization algorithm with the energy convergence criteria of 10^{-4} kcal/mol and force criteria of 5×10^{-3} kcal/mol/Å. *MD* was conducted using an *NVT* (constant-temperature, constant-volume) canonical ensemble at 298 K. The time step for *MD* was 1fs with a total simulation time of 500 ps (5×10^5 steps). The system temperature was controlled using a Berendsen Thermostat (0.1 ps decay constant). For the Radial Distribution Function (*RDF*) analysis, 500 ps of trajectory frames were used.

3. Result and discussion

3.1. Chemistry

3.1.2. Spectral data and physicochemical characterizations of compounds

5,6-anhydro-3-O-dodecyl-1,2-O-isopropylidene-α-D-glucofuranose ***(G-C$_{12}$)***

R $_{(\%)}$ 89; **Formula brute** $C_{21}H_{38}O_5$; **M** 370.54; $[\alpha]_D^{25}$ (CHCl$_3$) -41.7 (c = 0.7).

^{1}H NMR (300 MHz, DMSO-d6) (δppm): 0.87 (s, 3 H, CH_3), 3.62-3.85 (m, 31 H, CH_2-carbon chain), 1.25-1.51 (d, 6 H, 2 CH_3), 2.83-3.10-4.64-5.86 (d, 4 H, CH-glucose function). ^{13}C NMR (75 MHz, DMSO-d6) (δppm): 110.84 (2 $\underline{C}(CH3)2$), 22.07, 25.43 (2 $C(\underline{C}H_3)_2$), 13.91 (CH_3-carbon chain), 80.53-82.06 (CH-glucose function). 25.98-31.27 (CH-carbon chain).

*5,6-anhydro-3-O-hexyl-1,2-O-isopropylidene-α-D-glucofuranose (**G-C$_6$**)*

R $_{(\%)}$ **92;** Formula brute **$C_{15}H_{26}O_5$**; M **286.37;** $[\alpha]_D^{25}$ ($CHCl_3$) **-25.1 (c = 0.7).** **^{1}H:** δ_{ppm} 0.80 (s, 3 H, CH_3-carbon chain), 1.19-2.45 (s, 6 H, CH_2-carbon chain), 2.65-3.03 (s, 6 H, CH_3- glucose function), 3.42-3.80 (m, 4 H, $CH_{glucose}$), 5.79 (s, 1 H, CH $_{\text{glucose function}}$). **^{13}C:** δ_{ppm} 13.86 (CH_3-carbon chain), 22.05-26.51 (CH_2-carbon chain), 28.65-29.14 (CH_3-glucose function), 45.57-82.09 (CH-glucose function), 110.80 ($C\text{-}OH_{glucose}$).

3.2. Rheological Study

The viscosities of the two compounds ***G-C$_6$*** and ***G-C$_{12}$*** as a function of shear rate in the temperature range of 298-328 K as shown in **Figure 2**. The results derived from viscosity measurements demonstrate that ***G-C$_6$*** and ***G-C$_{12}$*** work as Newtonian liquids and their viscosities are independent to the shear rate from 0.01 to 200 s^{-1}. The evolutions of the viscosity for compounds ***G-C$_6$*** and ***G-C$_{12}$*** at different temperature permitted the estimate of the viscosity activation energy (E_a (kJ/mol)). The E_a values for ***G-C$_6$*** and ***G-C$_{12}$*** were calculated as follows [23].

$$\eta(T) = \eta_0 \exp\left(-\frac{E_a}{RT}\right) \quad (4)$$

Where Viscosity (η) (Pa.s), η_0 is a constant, R the gas constant (8.314 J/mol K) and T in K.

Arrhenius plots for the viscosity were given in **Figure 3**. Values of E_a for compound ***G-C$_6$*** and ***G-C$_{12}$*** were estimated from the slope of Ln (η) vs. 1/T. The activation energy for compounds ***G-C$_6$*** and ***G-C$_{12}$*** are respectively equal to 26.48 and 38.65, respectively. The results show that, the E_a for ***G-C*$_{12}$** is the highest. These energies are then grouped together in Table 1. We note that the higher the activation energy the higher the viscosity [23].

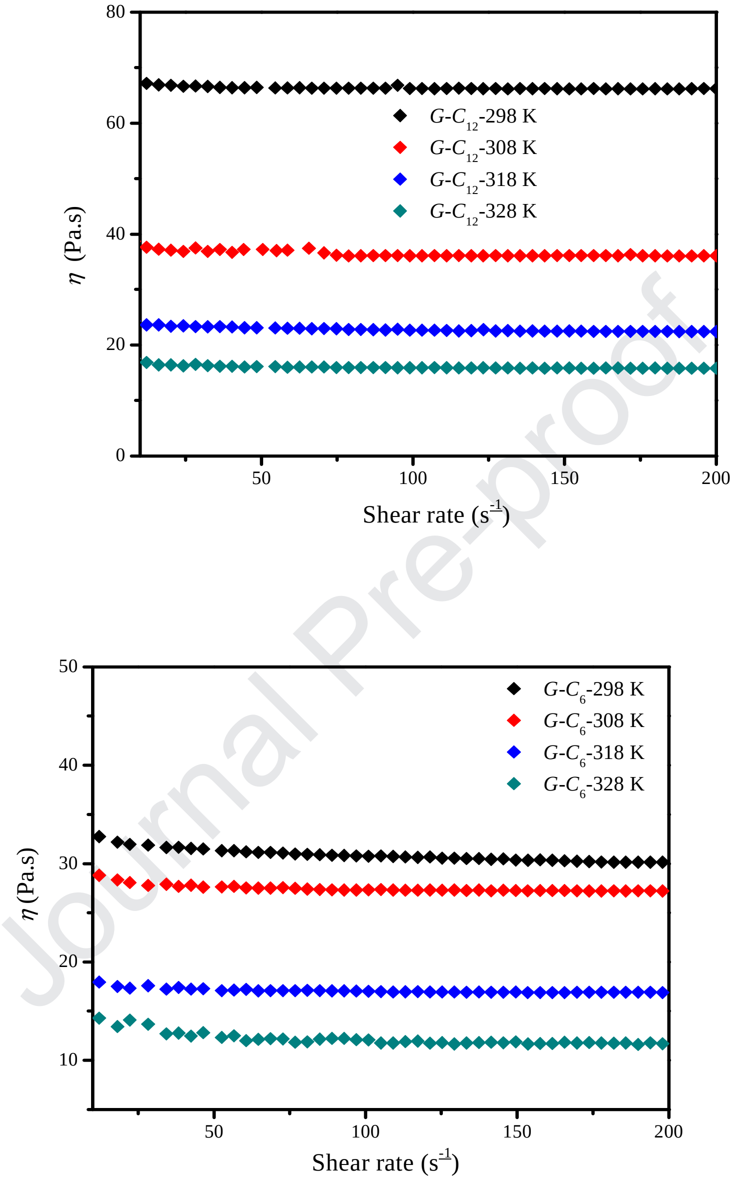

Figure 2. Viscosity measured as a function of shear for compounds ***G-C*$_6$** and ***G-C*$_{12}$** at different temperature.

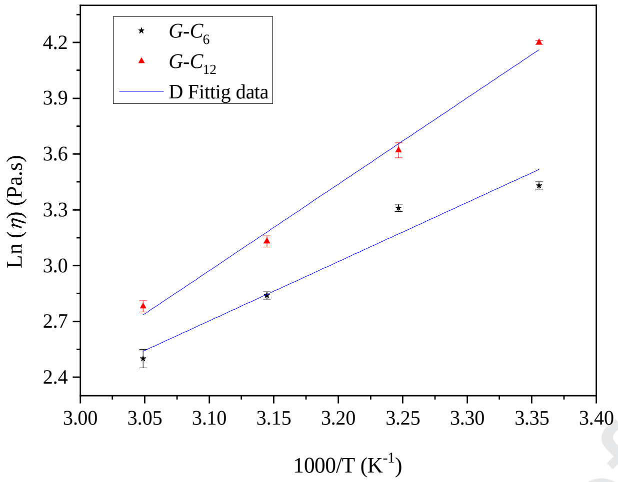

Figure 3. The relationship between Ln (*η*) and 1/T for compounds ***G-C$_6$*** and ***G-C$_{12}$*** at different temperature.

Table 1. Activation parameters for compounds ***G-C$_6$*** and ***G-C$_{12}$***.

	R^2	E_a (kJ/mol)
G-C$_6$	0.91948	26.48
G-C$_{12}$	0.99139	38.65

3.2. Electrochemical Study

3.2.1. PDP study

Polarization measurements have been carried out in order to gain knowledge concerning the kinetics of the anodic and cathodic reactions. Typical potentiodynamic polarization curves of the carbon steel in 1.0 M HCl solutions without and with the addition of different concentrations of ***G-C$_6$*** and ***G-C$_{12}$*** are shown in **Fig. 4.** Electrochemical kinetic parameters (corrosion potential (E_{corr}), corrosion current density (i_{corr}), cathodic and anodic Tafel slope (β_c and β_a), determined from these experiments by extrapolation method, are reported in **Table 2**.

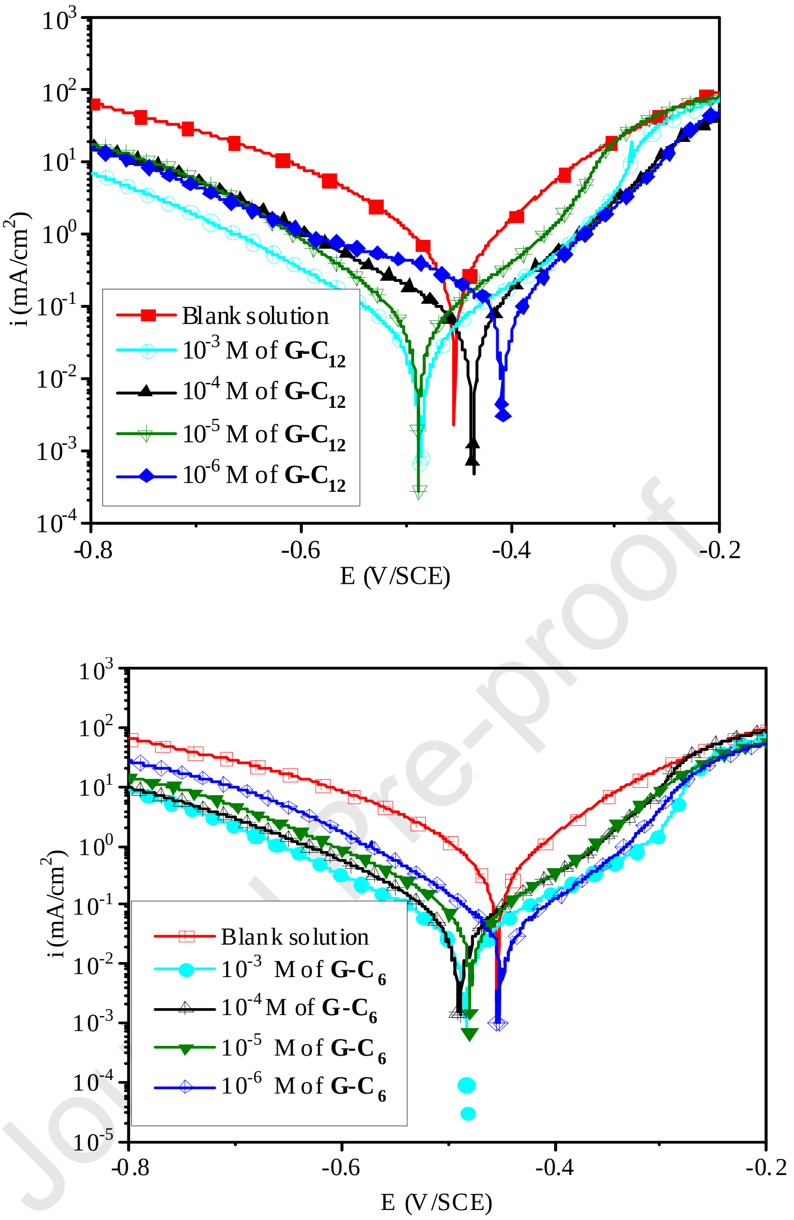

Figure 4. The polarization curves in the absence and in the presence of the compounds ***G-C$_6$*** and ***G-C$_{12}$***

Table 2. The values of the electrochemical parameters associated with the polarization study.

Medium	*Conc.* *(M)*	*-E$_{corr}$* *(mV vs. SCE)*	*i$_{corr}$* *(µA cm^{-2})*	*Tafel slopes* *(mV dec^{-1})*		*η$_{pp}$* *(%)*
				-β$_c$	*β$_a$*	
Blank	0	457.7	551.3	114.8	102.0	—
G-C$_{12}$	10^{-6}	405.8	79.7	168.8	76.0	85.5
	10^{-5}	486.3	77.7	109.3	95.6	85.9
	10^{-4}	485.9	46.4	133.2	67.6	91.6
	10^{-3}	420.3	17.4	114.5	44.3	96.8

G-C$_6$	10^{-6}	488.3	136.0	169.4	95.4	75.3
	10^{-5}	476.8	127.5	141.0	62.1	76.9
	10^{-4}	448.0	49.3	94.9	73.2	91.0
	10^{-3}	482.7	30.9	114.1	115.6	94.4

As it can be seen, the anodic and cathodic reactions are affected by the addition of ***G-C$_6$*** and ***G-C$_{12}$***. Thus, the addition of the inhibitor reduces the carbon steel dissolution as well as retards the hydrogen evolution reaction. In addition, the parallel cathodic Tafel curves in Fig. 4 show that the hydrogen evolution is activation-controlled and the reduction mechanism is not affected by the presence of the inhibitor [28]. The addition of the compounds causes a slight change in the corrosion potential values (E_{corr}) and the cathode slopes (β_c). Also, the difference between two successive values of corrosion potential lower than -85 (mV/SCE). This explains that the two compounds act as inhibitors of the mixed type [28]. Meanwhile, the inhibition degree for anodic reaction was lower than that for anodic reaction, implying the cathodic reaction was principally restrained.

The addition of the inhibitors (***G-C$_{12}$*** and ***G-C$_6$***.) causes a decrease in the corrosion current densities, hence an increase in inhibition efficiencies. The inhibitory efficiency is of the order of 96.8 %, 94.4 %, respectively for ***G-C$_{12}$*** and ***G-C$_6$***.

The order of efficiency (***G-C$_{12}$*** and ***G-C$_6$***) for the two compounds can be explained by the carbon chain (**-$C_{12}H_{25}$**) carried on the compound ***G-C$_{12}$***.

3.2.2. EIS study

Electrochemical impedance spectroscopy experiments were carried out on a newly polished steel surface in acidic solution without and with the addition of ***G-C$_{12}$*** and ***G-C$_6$***at open circuit potential at 298 K. **Fig. 5** show impedance spectra, as Nyquist and Bode plots obtained for carbon steel in the absence and the presence of different concentrations of ***G-C$_{12}$*** and ***G-C$_6$***. The Nyquist plots show a single depressed capacitive semicircle for both inhibited and uninhibited solutions, with one capacitive time constant in the Bode-phase plots. The depressed semicircle in Nyquist diagrams is characteristic of solid electrodes that exhibit frequency dispersion due to the roughness and other inhomogeneities of the surface [29]. Also, the slopes of the Bode-modulus plots (Log|Z| vs Log *f*) are not equal to -1 (Fig. 5), which are commonly observed for solid electrodes as a result of frequency dispersion of interfacial impedance. As the increase of inhibitor concentration, the radius of capacitive arc showed an uptrend, this was due to the surface of the steel was covered by more inhibitor molecules. That is to say, the compactness of protective film was improved as the inhibitor concentration increased.

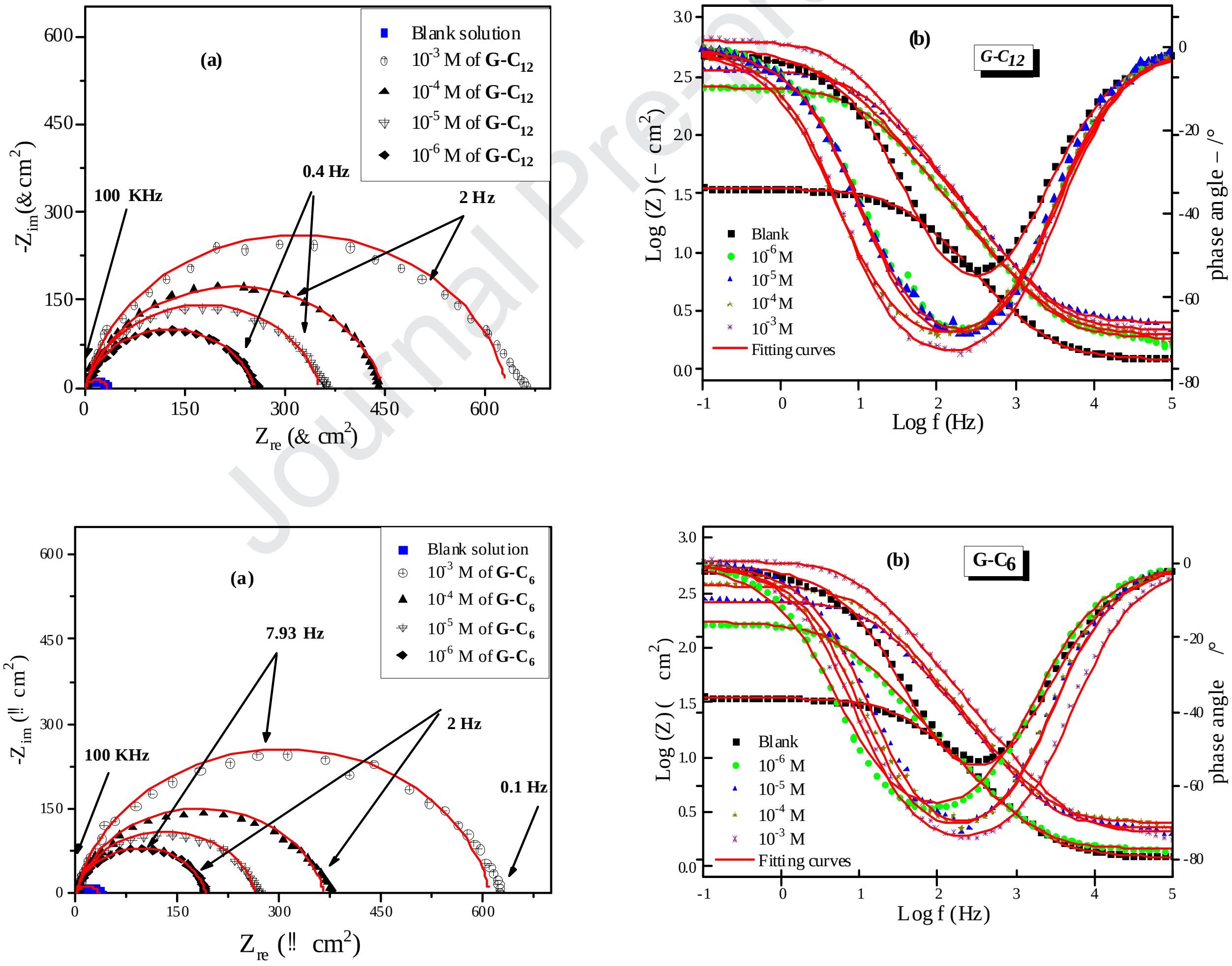

Figure 5. The steel curves obtained by impedance spectroscopy without and with the addition of ***G-C₁₂*** and ***G-C₆*** (**a**: Nyquist diagrams and **b**: Bode and phase plots).

The equivalent circuit model was fitted with a simple $R_s(R_p\text{CPE})$ electrical model due to one-time constant in the Bode phase plots and the result was shown in Figure SI2.

By statistics, the parameter was presented in **Table 3**. Among them, R_s was the solution resistance, R_p denoted the polarization resistance. CPE was the constant phase angle element, representing the capacitive property of electric double layer [30]. The CPE could be calculated by equation 5 [31]:

$$Z_{CPE} = \frac{1}{Y\left(jw\right)^{n}} \tag{5}$$

Thereinto, Y, w, j and n represent the CPE magnitude, angular frequency, imaginary root and error parameter, respectively. When the n was -1, 0, 0.5 and 1, the CPE could represent an inductor, resistor, Warburg impedance and capacitor, respectively. The C_{dl} was obtained from the equation 6 [32]:

$$C_{dl} = Y\left(2\pi f\right)^{n-1} \tag{6}$$

where f is the frequency at the maximum value of the imaginary part in EIS image. The n value could be used to reflect the surface roughness.

Table 3. The values of the electrochemical parameters associated with the impedance spectroscopy.

Comps	*C* (M)	R_s (Ω cm^2)	R_p (Ω cm^2)	C_{dl} (μFcm^{-2})	n_{dl}	*Q* (μF S^{n-1})	η_{EIS} %	θ
Blank	00	1.22±0.02	034.85±0.43	117.1	0.82±0.06	315.1±2.8	—	—
G-C₁₂	10^{-6}	1.83±0.03	254.10±0.44	60.03	0.85±0.05	112.0±0.5	86.3	0.863
	10^{-5}	2.50±0.06	351.10±0.44	44.83	0.86±0.05	079.4±1.2	90.1	0.901
	10^{-4}	1.98±0.02	446.90±0.44	30.32	0.83±0.05	063.0±0.5	92.2	0.922
	10^{-3}	2.17±0.02	633.20±0.43	24.67	0.84±0.05	048.0±0.5	94.4	0.944
G-C₆	10^{-6}	1.39±0.01	191.50±0.51	51.81	0.89±0.05	085.0±2.6	81.8	0.818
	10^{-5}	2.24±0.03	263.40±0.51	43.98	0.88±0.05	073.0±1.5	86.8	0.868
	10^{-4}	2.52±0.03	364.00±0.43	41.83	0.88±0.05	068.0±1.0	90.4	0.904
	10^{-3}	2.02±0.02	608.60±0.43	29.72	0.88±0.05	046.3±0.4	94.3	0.943

It can be seen that the n value in the blank solution was the lowest, indicating that the surface roughness was the highest. As the increase of inhibitor concentration, the n value presented a downtrend. This was due to the inhibitor adsorbed on the surface of steel and then decreased the surface homogeneity [33].

The examination of the results in **Table 3** indicating that the values of the polarization resistance (R_p) increase with the addition of the inhibitor compounds ***G-C$_{12}$*** and ***G-C$_6$*** that are attributed due to the adsorption of the compounds on to the metal surface [34]. Decreased in double layer capacity (C_{dl}) values in the presence of ***G-C$_{12}$*** and ***G-C$_6$*** are attributed due to the decrease in dielectric constant and the improvement of the thickness of the electrical double layer or the combination of both [34]. The inhibition efficiencies obtained in the study of impedance spectroscopy are of the following order of 94.4 % for the compound ***G-C$_{12}$*** and 94.3 % for the compound ***G-C$_6$***.The results obtained in the study of impedance confirm the results found in the potentiodynamic polarization (***G-C$_{12}$* > *G-C$_{12}$*)**.

3.2.3. Temperature effect, activation and adsorption parameters

The temperature is essential for the completeness of the studies of the carbon steel corrosion in the acidic medium, especially in the hydrochloric acid at a range of 238-328 K [35]. The results of the effect of temperature help us to calculate the several activation and adsorption parameters such as, activation energy (E_a), activation enthalpy (ΔH_a) entropy activation (ΔS_a) and adsorption entropy (ΔG°_{ads}). These activation and adsorption parameters give us more important information on the adsorption mechanism and the adsorption mode [35]. Figure SI3 show polarization curves at different temperatures range (238-328 K) without and with the addition of ***G-C$_{12}$*** and ***G-C$_6$***. Moreover, the parameters of temperature, activation and adsorption are given in **Table 4a**.

Table 4a. Temperature effect, activation and adsorption parameters

Temp (K)	$-E_{corr}$ *mV/SCE*	i_{corr} *μA/cm²*	$-\beta_c$ *mV dec*$^{-1}$	β_a *mV dec*$^{-1}$	η_{PDP} *%*	E_a *kJ mol*$^{-1}$	ΔH_a *kJ mol*$^{-1}$	ΔS_a *J mol*$^{-1}$ *K*$^{-1}$	$-\Delta G^{\circ}_{ads}$ *(kJ mol*$^{-1}$*)*
Blank									
298±2	496.3	551.3	43.4	39.0	—	35.44	32.84	-81.24	
308±2	491.0	1200	184.0	112.0	—	—	—	—	
318±2	475.0	1450	71.0	124.0	—	—	—	—	
328±2	465.0	2200	161.0	118.0	—	—	—	—	
G-C$_{12}$									-44.09
298±2	420.3	17.4	114.5	44.3	96.8	75.57	72.99	-25.90	
308±2	481.2	94.4	141.7	101.1	92.1	—	—	—	
318±2	464.4	120.5	158.9	73.9	91.7	—	—	—	
328±2	512.2	352.9	139.0	117.7	84.0	—	—	—	
G-C$_6$									-42.68
298±2	482.7	30.9	114.1	115.6	94.4	72.33	69.73	-18.70	
308±2	475.0	103.2	149.0	93.0	91.4	—	—	—	
318±2	504.2	272.2	139.8	79.7	81.2	—	—	—	
328±2	471.0	428.5	151.9	139.6	80.5	—	—	—	

Table 4a shows that the current density values increase with the addition of ***G-C$_{12}$*** and ***G-C$_6$*** compounds. Hence, a slight decrease in inhibition efficacy for both compounds, but still the two compounds remains effective at high temperature. The activation and adsorption parameters such as, activation energy of corrosion (E_a), activation enthalpy of corrosion (ΔH_a) entropy activation of corrosion (ΔS_a) and the standard Gibbs free energy of adsorption (ΔG°_{ads}) are calculated by the following equations (7-10) [36-39]

$$i_{corr} = A\exp\left(\frac{-E_a}{RT}\right) \tag{7}$$

$$i_{corr} = \frac{RT}{Nh}\exp\left(\frac{\Delta S_a}{R}\right)\exp\left(\frac{\Delta H_a}{RT}\right) \tag{8}$$

$$K_{ads} = \frac{1}{55.5}\exp\left(\frac{-\Delta G^{\circ}_{ads}}{RT}\right) \tag{9}$$

$$\frac{C_{inh}}{\theta} = \frac{1}{K_{ads}} + C_{inh} \tag{10}$$

The activation energy (E_a) was calculated by the variation of Ln (i_{corr}) = f ($1 / T$) (Figure SI4). ΔH_a and ΔS_a are also calculated by extrapolation of the Arrhenius equation and the variation of Ln (i_{corr} / T) = $1000 / T$ (Figure SI5). To obtain the best model to describe the adsorption of the inhibitor studied, the C_{inh}/θ curve as a function of the C_{inh} concentration of ***G-C$_{12}$*** and ***G-C$_6$*** must be linear, this shows an adsorption of ***G-C$_{12}$*** and ***G-C$_6$*** on the surface of steel. in 1.0 M HCl with a correlation coefficient greater than 0.9999 (Figure SI6).

From **Table 4a**, the activation energy values (E_a) for both compounds are larger than those of 1.0 M HCl. This explains the presence of an energy barrier involved after the addition of the compounds [40]. In addition, the positive values of the activation enthalpy (ΔH_a) in the presence of the *glucose*-derived compounds indicates inhomogeneity of the surface after addition of the compounds. Also, that the reaction is endothermic [40]. The most positive values of the entropy of activation (ΔS_a) show that the two inhibitors are well absorbed on the surface of the steel [41]. The standard Gibbs free energy of adsorption (ΔG°_{ads}) values for both compounds are greater than -40 kJ/mol. According to the literature, these two compounds are adsorbed on the surface of the steel by chemical mode of adsorption (chemisorption) [41]. **Table 4b** reports the type and corrosion mechanism inhibition for some selected 8-hydroxyquinoline derivatives recently used as corrosion inhibitors in hydrochloric acid medium compared with two newly syntheses compounds.

Table 4b. Inhibitors performance of novel quinoline derivatives used as corrosion inhibitors for mild steel in 1.0 M HCl medium from impedance spectroscopy measurements.

Compounds	*Materials*	*Inhibition Efficiency (*)*	*Adsorption isotherm*	*Inhibitor type*	*Ref.*
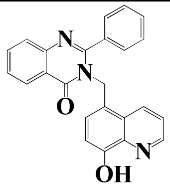	3-((8-hydroxyquinolin-5-yl)-methyl)-2-phenylquinazolin-4(3H)-one	94.4 %	Langmuir	Mixed type	[20]

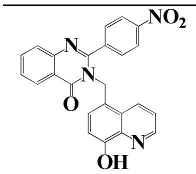	3-((8-hydroxyquinolin-5-yl)-2-(4-nitrophenyl)-quinazolin-4(3H)-one	95.9 %	Langmuir	Mixed type	[20]
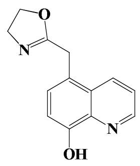	5-((4, 5-dihydro-oxazol-2-yl) methyl) quinolin-8-ol (QDO)	97.40 %	Langmuir	anodic type	[11]
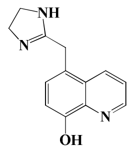	5-((4, 5-dihydro-imidazol-2-yl) methyl) quinolin-8-ol (QIM)	91.82 %	Langmuir	anodic type	[11]
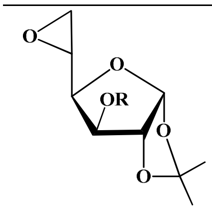 **R= C_6H_{13}, G-C_6**	5,6-anhydro-3-O-hexadecyl-1,2-O-isopropylidene-α-D-glucofuranose (G-C6)	94.4 %	Langmuir	Mixed type	This work
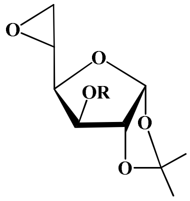 **R= $C_{12}H_{25}$, G-C_{12}**	5,6-anhydro-3-O-dodedecyl-1,2-O-isopropylidene-α-D-glucofuranose (G-C12)	96.8 %	Langmuir	Mixed type	This work

The glucose derivatives used in this study are ecological non-toxic and biodegradable because it is a natural origin (Glucose). In addition, our compound is more effective compared to the other compounds which is already published (**Table 4b**). However, the compounds used in this study are resistant to high temperature, which gives authorization for use in the industrial field.

4. Characterization of the metal surface

4.1. SEM study

We performed an *SEM* analysis to analyze and characterize the metal surface of the carbon steel after corrosion in molar hydrochloric acid with and without of the compounds. The *SEM* image in 1.0 M HCl alone shows that the surface is destroyed by corrosion (**Figure 6A**). The observation of the *SEM* images in the case of the presence of the glycoside compounds (**Figure 6B, C**) shows that the surface of the steel was protected by a layer of organic compounds in the form of a deposit [42,43].

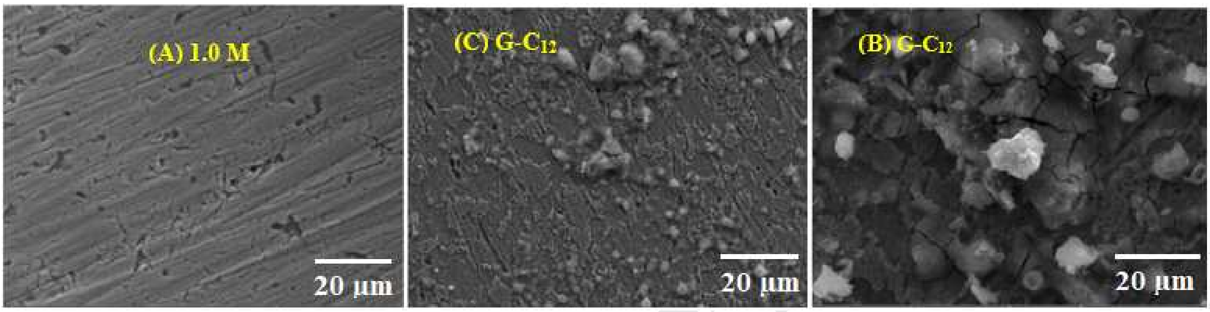

Figure 6. *SEM* image of *CS* before (A) and after immersion for 6 h in 1.0 M HCl with 10^{-3} M of (B) ***G-C$_{12}$*** and (C) ***G-C$_{6}$*.**

4.2. UV-visible spectroscopy

In order to study the complexing property of the two compounds with iron we have carried out a study by UV-visible spectroscopy (UV-vis) [44]. The UV-visible spectra shows that the maximum wavelengths move from 260.22 to 312.41 nm for the ***G-C$_{12}$*** compound and from 254.52 to 340.45 nm for the ***G-C$_{6}$***. This result reveals that the these two compounds are capable of making bonds with iron ions dissolved in 1.0 M HCl (Figure SI6).

4.3. ICP-OES analysis

To measure iron dissolution in HCl with and without inhibitors we performed an *ICP-OES* analysis. The analysis shows that there is an amount of iron of 259.939 mg/L in the case of carbon steel in 1.0 HCl alone. After the addition of the two compounds ***G-C$_{12}$*** and ***G-C$_{6}$*** it is observed that the amount of iron dissolved in HCl is of the order of 6.297 mg/L for the compound ***G-C$_{12}$*** and 6.312 mg/L for the compound ***G- C$_{6}$***.These results explain that the glycoside compounds decrease the iron dissolution in HCl, proves that the these two compounds have an inhibitory effect on the dissolution of the carbon steel in 1.0 M HCl [45].

5. Theoretical study

5.1. DFT

The adsorptive behavior of the *Epoxy Sugar* derivatives bearing a longer (-$C_{12}H_{25}$) or a shorter (-C_6H_{13}) alkyl chains can be evaluated through the shape and symmetry of the Highest Occupied Molecular Orbitals (*HOMO*) and Lowest Unoccupied Molecular Orbitals (*LUMO*), by analyzing [42,45]. *HOMO* designates the regions prone to electron donation (to electrophilic species), whereas *LUMO* the regions that have an affinity to accept the electrons (from nucleophile species). The distribution of *HOMO* in the studied *Epoxy sugar* derivatives (**Figure 7**) is delocalized mainly through the *oxygen* atoms of the *sugar* moiety, the similar distribution is observed also for *LUMO*, meaning that this part of molecule is where the interaction with the metals surface (iron) takes place by an electron donation from molecule toward the surface [46]. Electrostatic potential maps (*ESP*) presented in the **Figure 7c**, are helpful to pinpoint the rich (red color) or poor (blue) regions of electron density in the molecule. The regions with the high electron density are concentrated nearby oxygen atoms whereas the electron density distribution is low at the –C and –H atoms [47].

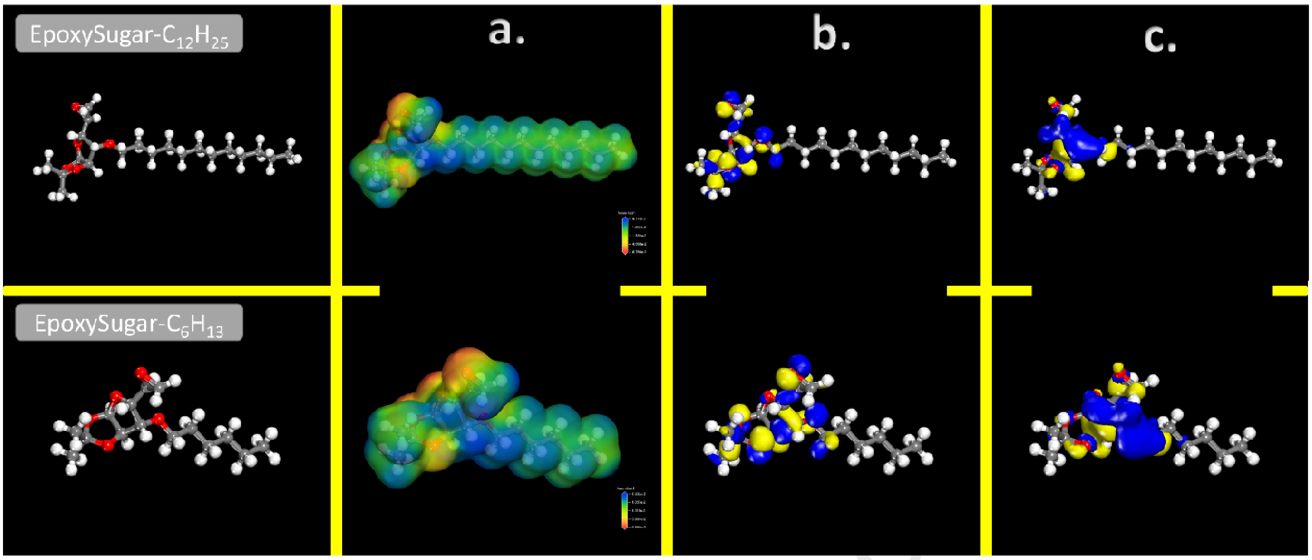

Figure 7. Optimized structures, distribution of orbitals (a. *HOMO* and b. *LUMO*) and *ESP* of *EpoxySugar* ***G-C***$_{12}$ and ***G-C***$_{6}$ molecules.

5.2. Monte Carlo

In the **Figure 8** are represented the resulting interaction energies curves for Fe (110) /***G-C***$_{12}$ or ***G-C***$_{6}$ /700 H_2O/$_{25}$ hydronium+25 chloride ions simulated corrosion media derived from Monte Carlo calculations. In each *MC* step there is a tendency of the convergence of every energy contribution (the total energy, the average total energy, the van der Waals energy, the electrostatic energy and the intermolecular energy) in the course of the calculation steps during the adsorption of the inhibitor molecule onto the Fe(110) surface [48].

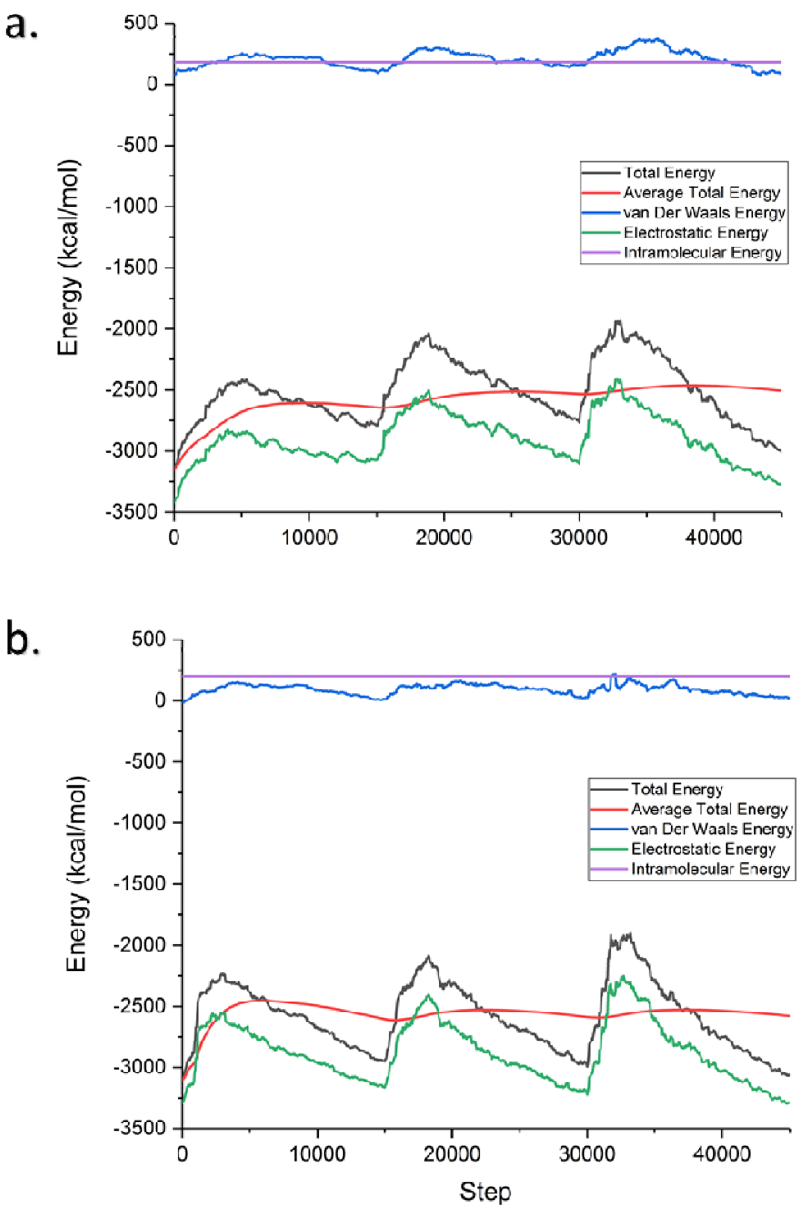

Figure 8. Monte Carlo calculation resulting interaction energies curves for Fe (110)/***G-C*$_{12}$** (a.) or ***G-C*$_{12}$** (b) /700 H_2O/25 hydronium+25 chloride ions simulated corrosion media.

The distribution of the adsorption energies during the Monte Carlo Calculations for the species that are used to simulate the corrosion media are represented in the **Figure 9**. The negative energy values are an indication of spontaneity of the inhibitor adsorption toward the Fe surface. The adsorption energy depending on the configuration of inhibitor onto the Fe surface for a ***G-C***$_{12}$ molecule is in the range of -83.55 to -139.45 kcal/mol, whereas the adsorption energy for ***G-C***$_{6}$ is in the range of -114.55 to -122.05 kcal/mol.

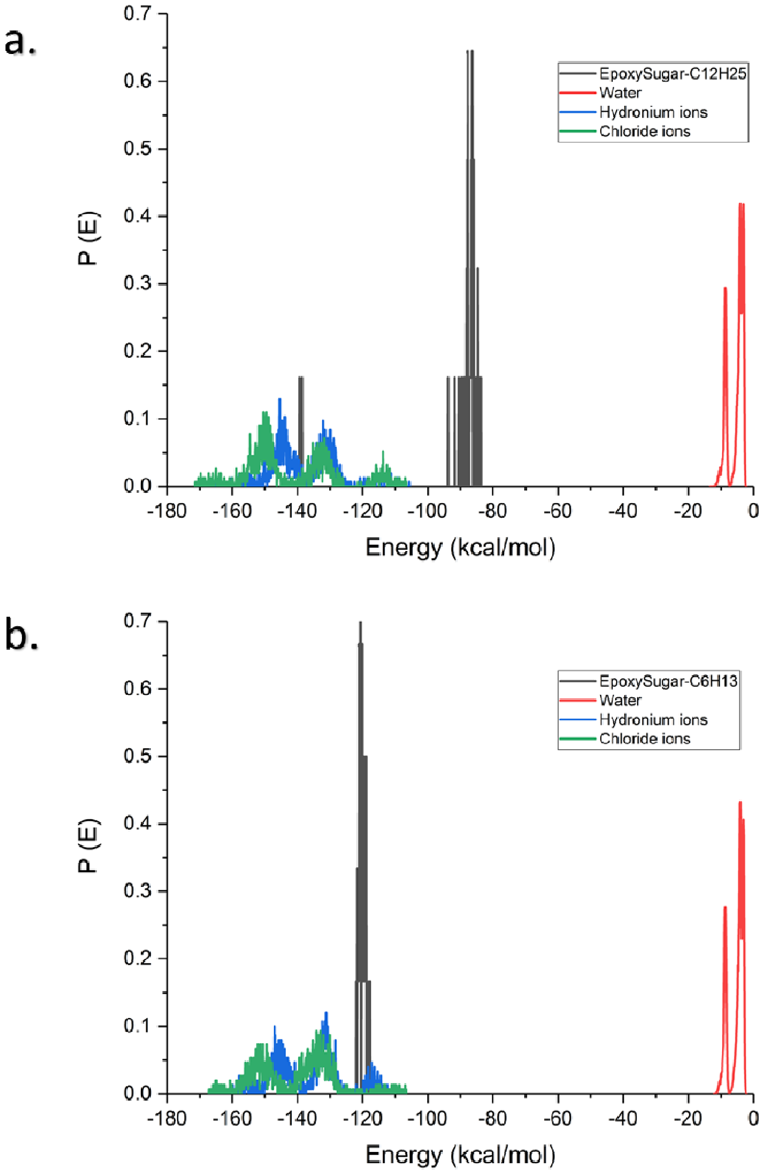

Figure 9. Adsorption energy distribution curves for Fe (110)/ ***G-C***$_{12}$ (a) or ***G-C***$_{6}$ (b) /700 H_2O/25 hydronium+25 chloride ions simulated corrosion media obtained via Monte Carlo calculations.

These relatively high adsorption energy values are accountable for the water displacement from Fe(110) surface due to the interaction of the inhibitor by electron sharing of its oxygen-sugar moiety and the metal surface. This interaction involves the overlap between the sharing of electrons from –O atoms of the inhibitor compounds and the 3d electrons of the iron surface [48].

5.6. Molecular Dynamics

In order to understand at the molecular level the interaction details of the studied inhibitor with the Fe (110) surface the Molecular Dynamics simulations were accomplished. The most stable geometry configurations (**Figure 10** a. and b) jointly with the *RDF* poses (**Figure 11**) obtained from these simulations provided a in depth information regarding the corrosion inhibition expressed by these *epoxy sugar* derivatives.

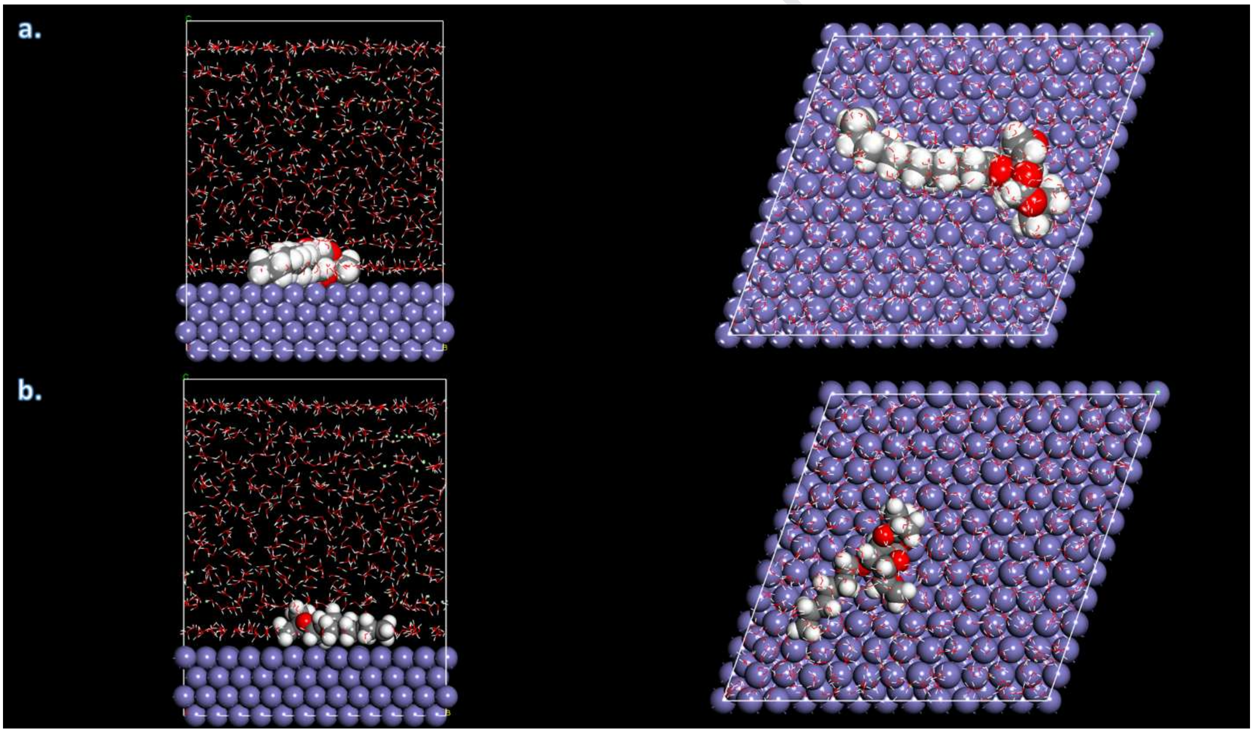

Figure 10. Side and top views of the most stable adsorption configuration for Fe (110)/***G-C***$_{12}$ (a.) or ***G-C***$_6$ (b.) /700 H_2O/25 hydronium+25 chloride ions in the simulated corrosion media obtained by Molecular Dynamics simulations.

Both of the inhibitors are flat lying onto the Fe surface, and somewhat a greater extent of adsorption energy (from *MC*) in the case of ***G-C$_{12}$*** compared to ***G-C$_6$*** is due to a greater surface of the former one.

The *RDF* is frequently used in *MD* simulations to evaluate the interaction between the studied inhibitors and the surface. When the peaks arise at the distances 1 Å up to 3.5 Å, it is associated with chemisorption (for the physisorption the peaks arise at the distances larger than 3.5 Å) [48]. The *RDF* value (**Figure 11**) for O atom of the both *epoxy sugar* derivatives shows that the bond length of O atoms and the iron surface is less than 3.5 Å, pointing out to chemisorptions through the inhibitors. This strong interaction leads to the protection of the metal against dissolution – by a chemisorption process.

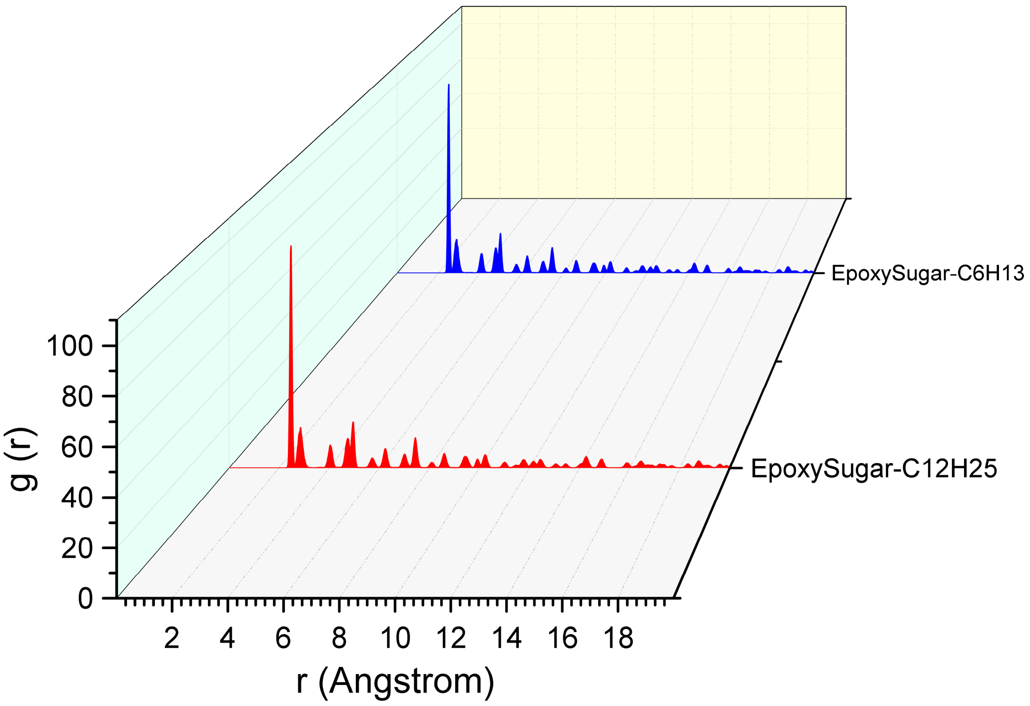

Figure 11. RDF of O atoms of the *Epoxy Sugar* derivatives on the Fe (110) surface.

6. Conclusion

In this study, we presented two ecological inhibitors as corrosion inhibitors of carbon steel. These compounds have been characterized by the usual spectral, the *NMR* analyzes show that it has good coherence between the spectral values and the assigned structures. In addition, the result of the electrochemical and rheological study shows that these two compounds have a remarkable corrosion inhibiting effect and that the inhibitory efficiency increases with the increase in concentrations for the two inhibitors. The highest inhibition efficiency values at 10^{-3} M (optimum concentration) are 94.4 % and 94.3 % for ***G-C*$_{12}$** and ***G-C*$_{6}$**, respectively. Both inhibitors acting on the metal surface as inhibitors of the mixed type. The corresponding values of the standard Gibbs free energy of adsorption (-44.09 to -42.68 kJ/mol) revealed that the adsorption mechanism of the ***G-C*$_{12}$** and ***G-C*$_{6}$** are mainly due to chemisorption. While, the increase in temperature causes a slight decrease in the values of the inhibitory efficiencies. Thermodynamic studies show that both inhibitors acting on the metal surface according to the Langmuir isotherm. Theoretical results DFT and MD simulation indicated that the both inhibitors is efficient, which is completely agree with the experimental results.

References

[1] P. Dohare, K.R. Ansari, M.A. Quraishi, I.B. Obot, Pyranpyrazole derivatives as novel corrosion inhibitors for mild steel useful for industrial pickling process: experimental and quantum chemical study, J. Ind. Eng. Chem. 52 (2017) 197-210.

[2] Y. Ye, D. Yang, H. Chen, S. Guo, Q. Yang, L. Chen, L. Wang, A high-efficiency corrosion inhibitor of N-doped citric acid-based carbon dots for mild steel in hydrochloric acid environment, J. Hazard. Mater. 381 (2020) 121019.

[3] M. Cui, S. Ren, H. Zhao, L. Wang, Q. Xue, Novel nitrogen doped carbon dots for corrosion inhibition of carbon steel in 1 M HCl solution, Appl. Surf. Sci. 443 (2018) 145-156.

[4] Y. Ye, Y. Zou, Z. Jiang, Q. Yang, L. Chen, S. Guo, H. Chen, An effective corrosion inhibitor of N doped carbon dots for Q235 steel in 1 M HCl solution, J. Alloys Compd. 815 (2020) 152338.

[5] A. Salhi, S. Tighadouini, M. El Massaoudi, M. Elbelghiti, A. Bouyanzer, S. Radi, S. El Barkany, F. Bentiss, A. Zarrouk, Keto-enol heterocycles as new compounds of

corrosion inhibitors for carbon steel in 1 M HCl: weight loss, electrochemical and quantum chemical investigation, J. Mol. Liq. 248 (2017) 340-349.

[6] Y. Ye, D. Yang, H. Chen, S. Guo, Q. Yang, L. Chen, H. Zhao, L. Wang, A high-efficiency corrosion inhibitor of N-doped citric acid-based carbon dots for mild steel in hydrochloric acid environment, J. Hazard. Mater. 381 (2020) 121019.

[7] N. Anusuya, J. Saranya, P. Sounthari, A. Zarrouk, S. Chitra, Corrosion inhibition and adsorption behavior of some bias-pyrimidine derivatives on mild steel in acidic medium, J. Mol. Liq. 225 (2017) 406-417.

[8] G. Bahlakeh, B. Ramezanzadeh, A. Dehghani, M. Ramezanzadeh, Novel cost-effective and high-performance green inhibitor based on aqueous Peganum harmala seed extract for mild steel corrosion in HCl solution: Detailed experimental and electronic/atomic level computational explorations, J. Mol. Liq. 283 (2019) 174-195.

[9] S.K. Mondal, S.R. Taylor, The Identification and Characterization of Organic Corrosion Inhibitors: Correlation of a Computational Model with Experimental Results, J. Electrochem. Soc. 161(10) (2014) C476-C485.

[10] K.F. Khaled, Understanding Corrosion Inhibition of Mild Steel in Acid Medium by Some Furan Derivatives: A Comprehensive Overview, J. Electrochem. Soc. 157(3) (2010) C116-C124.

[11] M. Rbaa, B. Lakhrissi, Novel oxazole and imidazole based on 8-Hydroxyquinoline as a Corrosion Inhibition of mild steel in HCl Solution: Insights from Experimental and Computational Studies, Surf. Interfaces 15 (2019) 43-59.

[12] O. Fergachi, F. Benhiba, M. Rbaa, M. Ouakki, M. Galai, R. Touir, M.E. Touhami, Corrosion Inhibition of Ordinary Steel in 5.0 M HCl Medium by Benzimidazole Derivatives: Electrochemical, UV–Visible Spectrometry, and DFT Calculations, Journal of Bio-and Tribo-Corrosion. 5 (1) (2019) 2-13.

[13] J. Fu, H. Zang, Y. Wang, S. Li, T. Chen, X. Liu, Experimental and theoretical study on the inhibition performances of quinoxaline and its derivatives for the corrosion of mild steel in hydrochloric acid, Ind, Eng. Chem. Res. 51 (18) (2012) 6377-6386.

[14] H. Soudeyns, X.I. Yao, Q.I.N.G. Gao, B. Belleau, B. Kraus, N.G.H.E. Nguyen-Ba, M.A. Wainberg, Anti-human immunodeficiency virus type 1 activity and in vitro toxicity of 2'-deoxy-3'-thiacytidine (BCH-189), a novel heterocyclic nucleoside analog, Antimicrob Agents Chemother. 35 (7) (1991) 1386-1390.

[15] X. Han, Y. Zhu, X. Yang, C. Li, Electrocatalytic activity of Pt doped TiO_2 nanotubes catalysts for glucose determination, J. Alloys Compd. 500 (2) (2010) 247-251.

[16] X. Zhang, Y. Xu, B. Ye, An efficient electrochemical glucose sensor based on porous nickel-based metal organic framework/carbon nanotubes composite (Ni-MOF/CNTs), J. Alloys Compd. 767 (2018) 651-656.

[17] N.A. Negm, N.G. Kandile, E.A. Badr, M.A. Mohammed, Gravimetric and electrochemical evaluation of environmentally friendly nonionic corrosion inhibitors for carbon steel in 1 M HCl, Corros. Sci. 65 (2012) 94-103.

[18] M. Finšgar, J. Jackson, Application of corrosion inhibitors for steels in acidic media for the oil and gas industry: a review, Corros. Sci. 86 (2014) 17-41.

[19] N. Asano, R.J. Nash, R.J. Molyneux, G.W. Fleet, Sugar-mimic glycosidase inhibitors: natural occurrence, biological activity and prospects for therapeutic application. Tetrahedron: Asymmetry, 11 (8) (2000) 1645-1680.

[20] B.E. Norman, A novel debranching enzyme for application in the glucose syrup industry, Starke. 34 (10) (1982) 340-346.

[21] R.A. Crittenden, M. Playne, Production, properties and applications of food-grade oligosaccharides, Trends Food Sci Technol. 7 (11) (1996) 353-361.

[22] M. Rbaa, M. Galai, F. Benhiba, I.B. Obot, H. Oudda, M.E. Touhami, A. Zarrouk, Synthesis and investigation of quinazoline derivatives based on 8-hydroxyquinoline as corrosion inhibitors for mild steel in acidic environment: experimental and theoretical studies, Ionics 2 (25) (2018)1-19.

[23] O. Dagdag, A. El Harfi, O. Cherkaoui, Z. Safi, N. Wazzan, L.Guo, R.T.Jalgham, Rheological, electrochemical, surface, DFT and molecular dynamics simulation studies on the anticorrosive properties of new epoxy monomer compound for steel in 1 M HCl solution, RSC Adv. 9 (8) (2019) 4454-4462.

[24] V. V. Mehmeti, A. R. Berisha, Corrosion Study of Mild Steel in Aqueous Sulfuric Acid Solution Using 4-Methyl-4H-1,2,4-Triazole-3-Thiol and 2-Mercaptonicotinic Acid—An Experimental and Theoretical Study, Front. Chem. 5 (61) (2017) 1-12.

[25] A. Berisha, C.Combellas, F.Kanoufi, P.Decorse, N.Oturan, J. Médard, J. Pinson, Some theoretical and experimental insights on the mechanistic routes leading to the spontaneous grafting of gold surfaces by diazonium salts, Langmuir 33 (35) (2017) 8730-8738.

[26] A. Berisha, The influence of the grafted aryl groups on the solvation properties of the graphyne and graphdiyne-a MD study, OPEN CHEM. 17 (1) (2019) 703-710.

[27] M. Bhardwaj, R. Balasubramaniam, Uncoupled non-linear equations method for determining kinetic parameters in case of hydrogen evolution reaction following Volmer–Heyrovsky–Tafel mechanism and Volmer–Heyrovsky mechanism, Int. J. Hydrogen Energy. 33 (9) (2008) 2178-2188.

[28] Y. Qiang, S. Zhang, B. Tan, S. Chen, Evaluation of Ginkgo leaf extract as an eco-friendly corrosion inhibitor of X70 steel in HCl solution, Corros. Sci. 133 (2018) 6-16.

[29] H. Shih, F. Mansfeld, A fitting procedure for impedance data of systems with very low corrosion rates, Corros. Sci. 29 (1989) 1235-1240.

[30] G. Sığırcık, D. Yildirim, T. Tüken, Synthesis and inhibitory effect of N,N'-bis(1-phenylethanol)ethylenediamine against steel corrosion in HCl Media, Corros. Sci. 120 (2017) 184-193.

[31] Y. Qiang, S. Zhang, S. Yan, X. Zou, S. Chen, Three indazole derivatives as corrosion inhibitors of copper in a neutral chloride solution, Corros. Sci. 126 (2017) 295-304.

[32] M. Ramezanzadeh, G. Bahlakeh, Z. Sanaei, B. Ramezanzadeh, Corrosion inhibition of mild steel in 1 M HCl solution by ethanolic extract of eco-friendly Mangifera indica (mango) leaves: Electrochemical, molecular dynamics, Monte Carlo and ab initio study, Appl. Surf. Sci. 463 (2019) 1058-1077.

[33] M. Rbaa, F. Benhiba, I.B. Obot, H. Oudda, I. Warad, B. Lakhrissi, A. Zarrouk, Two new 8-hydroxyquinoline derivatives as an efficient corrosion inhibitors for mild steel in hydrochloric acid: Synthesis, electrochemical, surface morphological, UV–visible and theoretical studies, J. Mol. Liq. 12 (276) (2018) 120-133.

[34] M. Rbaa, H. Lgaz, Y. El Kacimi, B. Lakhrissi, F. Bentiss, A. Zarrouk, Synthesis, characterization and corrosion inhibition studies of Novel 8-Hydroxyquinoline derivatives on the acidic corrosion of mild steel: Experimental and computational studies, Mater Discover. 12 (2018) 43-54.

[35] M. El Faydy, M. Galai, A. El Assyry, A. Tazouti, R. Touir, B. Lakhrissi, M. Ebn Touhami, A. Zarrouk, Experimental investigation on the corrosion inhibition of carbon steel by 5-(chloromethyl)-8-quinolinol hydrochloride in hydrochloric acid solution, J. Mol. Liq. 219 (2016) 396-404.

[36] H. Tayebi, H. Bourazmi, B. Himmi, A. El Assyry, Y. Ramli, A. Zarrouk, A. Geunbour, B. Hammouti and E.E. Ebenso, An electrochemical and theoretical evaluation of new quinoline derivative as a corrosion inhibitor for carbon steel in HCl solutions, Der Pharm. Lett. 6 (6) (2014) 20-34.

[37] A. Zarrouk, H. Zarrok, Y. Ramli, M. Bouachrine, B. Hammouti, A. Sahibed-dine and F. Bentiss, Inhibitive properties, adsorption and theoretical study of 3,7-dimethyl-1-(prop-2-yn-1-yl)quinoxalin-2(1H)-one as efficient corrosion inhibitor for carbon steel in hydrochloric acid solution, J. Mol. Liq. 222 (2016) 239-252.

[38] A Zarrouk, B. Hammouti, H. Zarrok, R. Salghi, A. Dafali, Lh. Bazzi, L. Bammou, S. S. Al-Deyab, Electrochemical impedance spectroscopy and weight loss study for new pyridazine derivative as inhibitor for copper in nitric acid, Der Pharma Chem. 4(1) (2012) 337-346.

[39] O. Fergachi, F. Benhiba, M. Rbaa, R. Touir, M. Ouakki, M. Galai, B. Lakhrissi, H. Oudda, M. E. Touhami, Experimental and Theoretical Study of Corrosion Inhibition of Mild Steel in 1.0 M HCl Medium by 2(-4(hloro phenyl-1H- benzo[d]imidazol)-1-yl)phenyl)methanone, Mat. Res. 6 (21) (2018) 1516-1439.

[40] M. Ouakki, M. Rbaa, M. Galai, B. Lakhrissi, E.H. Rifi, M. Cherkaoui, Experimental and Quantum Chemical Investigation of Imidazole Derivatives as Corrosion Inhibitors on Mild Steel in 1.0 M Hydrochloric Acid, Journal of Bio-and Tribo-Corrosion. 4 (3) (2018) 35.

[41] M. Rbaa, M. Galai, Y. El Kacimi, M. Ouakki, R. Touir, B. Lakhrissi, M.E. Touhami, Adsorption Properties and Inhibition of Carbon Steel Corrosion in a Hydrochloric Solution by 2-(4, 5-diphenyl-4, 5-dihydro-1h-imidazol-2-yl)-5-methoxyphenol, Port. Electrochim. Acta 35 (6) (2017) 323-338.

[42] M. Rbaa, N. Errahmany, Y. El Kacimi, M. Galai, M. El Faydy, Y. Lakhrissi, B. Lakhrissi, Chemical and Electrochemical Studies of Novel Quinazolinone Derivatives based on 8-hydroxyquinoline as Corrosion Inhibitor for Mild Steel in 1.0 M HCl Solution. Anal. Bioanal. Electrochem. 10 (10) (2018) 1328-1354.

[43] M. Rbaa, M. Galai, M. El Faydy, Y. El Kacimi, M. Ebn Touhami, A. Zarrouk, B. Lakhrissi, Synthesis and Characterization of New Benzimidazoles Derivatives of 8-hydroxyquinoline as a Corrosion Inhibitor for Mild Steel in 1.0 M Hydrochloric Acid Medium, Anal. Bioanal. Electrochem. 9 (7) (2017) 904-928.

[44] C. Gabler, C. Tomastik, J. Brenner, L. Pisarova, N. Doerr, G. Allmaier, Corrosion properties of ammonium based ionic liquids evaluated by SEM-EDX, XPS and ICP-OES, Green Chem. 13 (10) (2011) 2869-2877.

[45] A. Zarrouk, B. Hammouti, A. Dafali, M. Bouachrine, H. Zarrok, S. Boukhris, S.S. Al-Deyab, A theoretical study on the inhibition efficiencies of some quinoxalines as corrosion inhibitors of copper in nitric acid, J. Saudi Chem. Soc. 18 (2014) 450-455.

[46] N.O. Eddy, Experimental and theoretical studies on some amino acids and their potential activity as inhibitors for the corrosion of mild steel, part 2, J. Adv. Res. 2(1) (2011) 35-47.

[47] R. Hsissou, O. Dagdag, S. Abbout, F. Benhiba, M. Berradi, M. El Bouchti, A. Elharfi, Novel derivative epoxy resin TGETET as a corrosion inhibition of E24 carbon steel in 1.0 M HCl solution. Experimental and computational (DFT and MD simulations) methods, J. Mol. Liq. 284 (15) (2019) 182-192.

[48] C. Verma, E.E. Ebenso, I. Bahadur, I.B. Obot, M.A. Quraishi, 5-(Phenylthio)-3H-pyrrole-4-carbonitriles as effective corrosion inhibitors for mild steel in 1 M HCl: experimental and theoretical investigation, J. Mol. Liq. 212 (2015) 209-218.

Highlights

- Newly both glucose derivatives was synthesized and evaluated as corrosion inhibitor for steel in acidic medium.
- Adsorption of G-C_{12} and G-C_6, obeyed the Langmuir adsorption isotherm model their adsorption was supported by SEM and UV-vis spectroscopic analyses.
- The experimental results were correlated with DFT and MC stimulation results.

Dear Editor-in-Chief,

This statement is to certify that all Authors of the article **“Epoxy sugar based glucose derivatives as eco friendly corrosion inhibitors for the carbon steel in hydrochloric acid medium: Synthesis, rheological, electrochemical and theoretical investigations”** have been seen and approved the manuscript being submitted. We warrant that the article is the Auhor’s original work. We warrant that the article has not received prior publication and is not under consideration for publication elsewhere. No conflict of interest exists, or if such conflict exists, the exact nature must be declared. On behalf of all Co-Authors, the corresponding Author shall bear full responsibility for the submission.

All Authors agree that author list is correct in its content and order and that no modification to the author list can be made without the formal approval of the Editor-in-Chief, and all Authors accept that the Editor-in-Chief’s decisions over acceptance or rejection.